Chemistry & Biology
Article

Structure-Activity-Based Design of a Synthetic Malaria Peptide Eliciting Sporozoite Inhibitory Antibodies in a Virosomal Formulation

Shinji L. Okitsu,[1] Ursula Kienzl,[2] Kerstin Moehle,[2] Olivier Silvie,[3,7] Elisabetta Peduzzi,[1] Markus S. Mueller,[1] Robert W. Sauerwein,[4] Hugues Matile,[5] Rinaldo Zurbriggen,[6] Dominique Mazier,[3] John A. Robinson,[2] and Gerd Pluschke[1,*]

[1] Molecular Immunology, Swiss Tropical Institute, CH-4002 Basel, Switzerland
[2] Institute of Organic Chemistry, University of Zurich, CH-8057 Zurich, Switzerland
[3] Inserm U511, Immunobiologie Cellulaire et Moléculaire des Infections Parasitaires, Centre Hospitalo-Universitaire Pitié-Salpêtrière, Université Pierre et Marie Curie, 75013 Paris, France
[4] Department of Medical Microbiology, University Medical Centre St Radboud, 6500HB Nijmegen, The Netherlands
[5] F. Hoffmann La Roche Ltd., CH-4070 Basel, Switzerland
[6] Pevion Biotech Ltd., CH-3018 Bern, Switzerland
[7] Present address: Department of Parasitology, Heidelberg University School of Medicine, Im Neuenheimer Feld 324, 69120 Heidelberg, Germany.
*Correspondence: gerd.pluschke@unibas.ch
DOI 10.1016/j.chembiol.2007.04.008

SUMMARY

The circumsporozoite protein (CSP) of *Plasmodium falciparum* is a leading candidate antigen for inclusion in a malaria subunit vaccine. We describe here the design of a conformationally constrained synthetic peptide, designated UK-39, which has structural and antigenic similarity to the NPNA-repeat region of native CSP. NMR studies on the antigen support the presence of helical turn-like structures within consecutive NPNA motifs in aqueous solution. Intramuscular delivery of UK-39 to mice and rabbits on the surface of reconstituted influenza virosomes elicited high titers of sporozoite cross-reactive antibodies. Influenza virus proteins were crucially important for the immunostimulatory activity of the virosome-based antigen delivery system, as a liposomal formulation of UK-39 was not immunogenic. IgG antibodies elicited by UK-39 inhibited invasion of hepatocytes by *P. falciparum* sporozoites, but not by antigenically distinct *P. yoelii* sporozoites. Our approach to optimized virosome-formulated synthetic peptide vaccines should be generally applicable for other infectious and noninfectious diseases.

INTRODUCTION

Malaria is the most important parasitic disease in people and may cause as many as 2.5 million deaths per annum [1]. Vaccine development against both *Plasmodium falciparum* and *P. vivax* is ongoing [2], and one candidate vaccine, RTS,S/AS02A, demonstrated 30% protection against the first episode of malaria and 58% protection against severe malaria in a clinical trial in Mozambican children [3]. Nevertheless, it is assumed that it will take at least another decade until a malaria vaccine will be available that is more effective and more cost effective than current malaria control tools, such as insecticide-treated bednets and intermittent preventive treatment in infants [4–6].

Apart from plans to develop a radiation-attenuated sporozoite vaccine [7], vaccine development against malaria is focusing largely on subunit vaccine technologies [8]. It is thought that an effective malaria subunit vaccine will have to incorporate antigens against several developmental stages of the parasite. A combination of actions against sporozoites, infected liver cells, merozoites, and infected red blood cells may be required to achieve substantial protective activity [8]. The fact that most vaccines currently available are based on attenuated or inactivated whole pathogens or material derived directly from them demonstrates that the technological problems associated with peptide and protein subunit vaccine design are still incompletely solved. Major obstacles include difficulties in retaining the native conformation of key antibody epitopes and the need for an effective but safe human-compatible exogenous adjuvant in order to achieve efficient immune responses [9].

We are addressing the problem of protein subunit vaccine design by developing synthetic peptide structures that elicit antibodies against surface epitopes of native malaria antigens [10–12] and coupling them to the surface of immunopotentiating reconstituted influenza virosomes (IRIVs) as a liposomal carrier system [12, 13]. IRIVs are spherical, unilamellar vesicles, prepared by detergent removal from a mixture of natural and synthetic phospholipids and influenza surface glycoproteins. The hemagglutinin membrane glycoprotein of the influenza virus is a

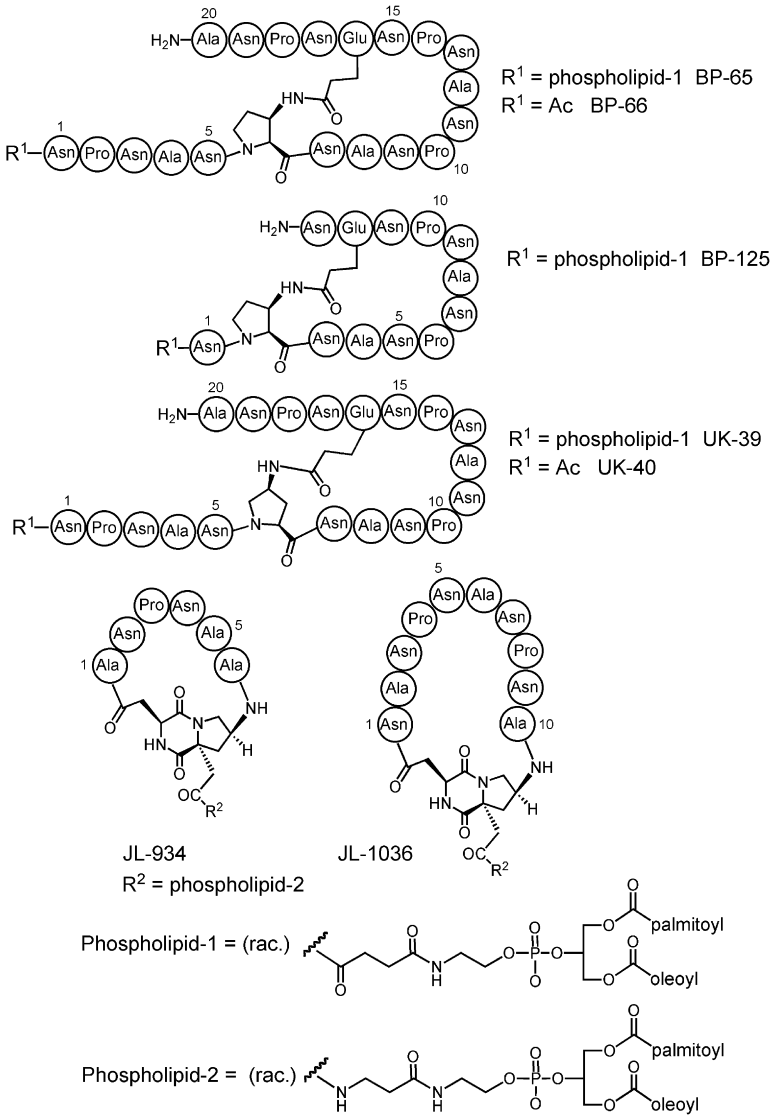

Figure 1. Structures of Peptidomimetics Discussed in the Text

fusion-inducing component, which facilitates antigen delivery to immunocompetent cells. IRIVs represent a universal antigen delivery system for multicomponent subunit vaccines, as antigens can be either attached to their surface to elicit antibody responses or encapsulated in their lumen to elicit CD8 T cell responses. They have an excellent safety profile and are already registered for human use [14].

Sequential rounds of optimization of synthetic peptide structures, as typically applied in drug research, may ideally lead to vaccine candidate antigens which elicit primarily or exclusively antibodies that contribute to immune protection. In the case of the central repeat region $(NPNA)_{\approx 37}$ of the circumsporozoite protein (CSP) of *P. falciparum* sporozoites, results of clinical trials with a linear $(NANP)_3$ peptide conjugated to tetanus toxin in alum [15] were disappointing. We have previously described the synthesis and immunological properties of template-bound NPNA peptides, which were superior to their linear counterparts in eliciting sporozoite-binding antibodies [12]. Building on NMR and modeling studies, we designed and synthesized an improved cyclic NPNA-repeat region peptide (designated BP-65), which has been shown to efficiently elicit anti-sporozoite antibody responses in mice [11]. Here we describe functional properties of monoclonal antibodies (mAbs) elicited by BP-65, and the properties and preclinical profiling of a synthetically more accessible derivative (UK-39). An IRIV-based formulation of this peptide, designated PEV302, is currently being tested in human clinical trials.

RESULTS

Sporozoite-Inhibitory Activity of Anti-BP-65 mAbs

Two mAbs (designated EP3 and EP9) specific for the synthetic compound BP-65 (Figure 1) were generated from spleen cells of influenza-primed mice immunized with BP-65-loaded IRIVs. Both mAbs bind to *P. falciparum*

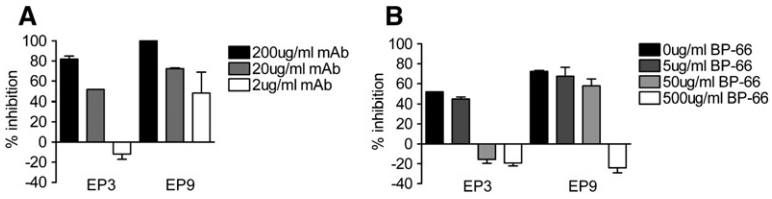

Figure 2. Hepatocyte Invasion Inhibition by Anti-BP-65 mAbs

(A) Inhibition of parasite invasion into primary human hepatocytes by mAb EP3 and mAb EP9. Shown is the mean percentage of inhibition compared to a PBS control ± SD for duplicates.

(B) Competition of invasion inhibition by increasing concentrations of BP-66 peptide (BP-65 without PE). Inhibitory mAbs were used at a constant concentration of 20 μg/ml.

sporozoites in immunofluorescence assays (IFAs), and functional inhibitory activity was assessed by performing in vitro invasion inhibition assays with *P. falciparum* sporozoites and primary human hepatocytes. At a concentration of 200 μg/ml, mAb EP3 caused 82% and mAb EP9 100% invasion inhibition (Figure 2A). The inhibitory activity decreased in a dose-dependent manner when increasing concentrations of BP-66 were added to the antibody-parasite mixture (Figure 2B), confirming the specificity of the inhibitory activity of the mAbs.

Design of UK-40 and Its Phosphatidylethanolamine Conjugate UK-39

In an attempt to minimize the size of the synthetic vaccine antigen, a derivative of BP-65, called BP-125, without the C-terminal PNA and N-terminal NPNA portions, was produced and tested for reactivity with the sporozoite-inhibitory anti-BP-65 mAbs EP3 and EP9. Only a strongly diminished reactivity was observed (see Figure S1 in the Supplemental Data available with this article online), indicating that BP-65 represents the minimal essential structure.

In BP-65, the folded conformation of the peptide is stabilized by crosslinking an amino group at the β position of Pro^6 to a spatially adjacent side-chain carboxyl of Glu as a replacement for Ala^{16} [11]. As limited availability of orthogonally protected (2S,3R)-3-aminoproline required for the synthesis of BP-65 represented an obstacle for upscaling of the synthesis for clinical-grade material, we synthesized derivatives of BP-65 designated UK-40 and UK-39 (phosphatidylethanolamine [PE] conjugate of UK-40), in which this building block is replaced by (2S,4S)-4-aminoproline (Figure 1). The required orthogonally protected N(α)-Fmoc(2S,4S)-4-(Boc)aminoproline ([2S,4S]-Boc-4-amino-1-Fmoc-pyrrolidine-2-carboxylic acid) is commercially available.

NMR Studies of UK-40

The solution structure of UK-40 was investigated in water (90% H_2O, 10% D_2O [pH 5.0], 293K) by ^1H NMR spectroscopy. The ^1H NMR spectrum of UK-40 indicated the existence of a major and two minor forms in a ratio of 14:3:1 which interconvert slowly on the NMR timescale, caused by *cis-trans* isomerism at Asn-Pro peptide bonds. Similar *cis-trans* rotamers were found in BP-66 in earlier work [11] and in linear peptides containing multiple NPNA repeats [16]. The major form can be assigned the all-*trans* conformation on the basis of observed nuclear Overhauser effect (NOE) connectivities. Resonance overlap prevented an assignment of the minor forms to specific peptide-bond rotamers. Chemical-shift assignments for the major rotamer (Table S1) were made using standard 2D NMR methods [17]. Side-chain proton frequencies in UK-40 exhibited major spectral overlap, although this problem was not as severe as seen in linear peptides containing multiple tandem NPNA repeats. This is illustrated in Figure S2, where HN-C(α)H crosspeaks from 2D DQF-COSY spectra are shown for UK-40 and the peptide Ac-$(NPNA)_3$-NH_2. Notable in the spectrum of UK-40 are the significantly upfield shifted amide HN resonances of Asn^9 and Ala^{12}. The amide proton chemical-shift temperature coefficients were measured and are given in Figure S3. Notable are the low values for both Ala^8 and Asn^9, suggesting that both these amide NHs are involved in intramolecular hydrogen bonding. A low value is also seen for Ala^{12}, but not for Asn^{13}.

Two-dimensional NOESY spectra of UK-40 showed d_{NN} (i, i + 1) NOE connectivities between amide protons of Asn_{i+3}, Ala_{i+4}, and Asn_{i+5} within each NAN motif, as shown in Figure S3. The same pattern of NOE interactions was also found earlier in BP-66 [11]. Furthermore, characteristic medium-range $d_{\alpha N}$ (i, i + 2) NOEs were found between Asn^7 and Asn^9, Asn^9 and Asn^{11}, Pro^{10} and Ala^{12}, and Pro^{14} and Glu^{16} in UK-40. Weak NOE contacts between side chains of the first Asn and the Ala of each NPNA motif are also seen, as predicted in the structure model of an NPNA motif in a helical turn conformation (vide infra) (Figure 3A). No other medium-/long-range NOEs were observed in NOESY spectra.

Using the available short- and medium-range NOE connectivities, average solution structures for UK-40 were calculated using DYANA. The final ensemble of 20 structures (see Table S2) is shown in Figure 3B. The backbone atoms of residues 6–16 enclosed within the macrocyclic ring can be superimposed with a root-mean-square deviation of 1.6 Å, whereas the remaining residues at the N and C termini show much greater conformational diversity. When each tetrapeptide motif within the macrocycle is considered, the highest structural similarity both to the ANPNA crystal structure [18] and to a model helical turn conformation is seen in the first (N^5-A^8) and in particular the central (N^9-A^{12}) tetrapeptide motifs (Figure 4), suggesting that helical turns are significantly populated in this portion of the molecule. Within the third unit N^{13}-E^{16}, however, the helical turn conformations are adopted much less frequently, or not at all, in the 20 lowest-energy

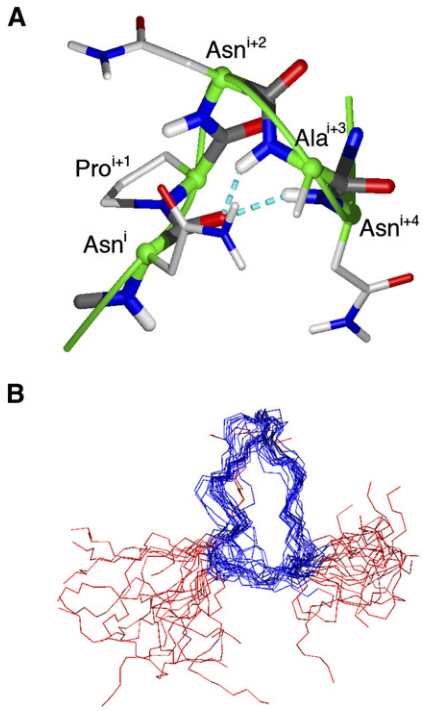

Figure 3. Structural Analysis of UK-40

(A) An NPNA motif is depicted in a helical turn conformation (see text). N atoms, dark blue; O atoms, red; C atoms, gray; amide H atoms, light white; H bonds, pale blue broken line. Here the first Asn has ϕ/ψ angles in the β region, and the following Pro, Asn, and Ala in the α region. A green ribbon traces the backbone.

(B) Superimposition of the final 20 DYANA structures for UK-40. The backbone only is represented, superimposed using all backbone atoms from Apro6 to Glu16 (region in blue).

DYANA structures, suggesting either that the turn is not significantly populated or, as seems more likely, that the average NMR structures do not represent accurately these regions of the macrocycle due to the presence of multiple rapidly interconverting helical and extended conformations. The low number and weak intensity of many NOEs are indicative of significant backbone flexibility. Moreover, the occurrence of significant restraint violations, such as from the Glu^{16} C(α)H to Asn^{17} HN NOE, indicates also the presence of extended (β) chain forms.

Antigenic Properties

The antigenic properties of virosomally formulated UK-39 were compared to those of BP-65 [11] and two previously described [12] template-bound peptides (JL-934 and JL-1036) (see Figure 1). Panels of CSP-repeat region-specific sporozoite-binding mAbs obtained after immunization of mice with either NPNA peptides or with *P. falciparum* sporozoites were tested in ELISA for crossreactivity with first- to fourth-generation compounds (Table 1). The results demonstrate that antibodies with a range of different fine specificities can bind to native CSP on the sporozoite surface. Thus, mAb 1.26, the only sporozoite crossreactive mAb elicited by the antigen JL-934 [12], did not bind to the other peptide antigens, and only three of the four sporozoite-binding mAbs elicited by the peptide antigen JL-1036 [12] crossreacted with the antigens BP-65 and UK-39. The two mAbs elicited by virosomal formulations of BP-65 both recognized sporozoites and UK-39, whereas only one mAb (EP9) recognized JL-1036 and none JL-934. Crossreactivity analysis with a set of 12 CSP-repeat region-specific mAbs raised against *P. falciparum* sporozoites demonstrated that only 2 of these mAbs crossreacted with JL-934, 5 with JL-1036, and all 12 with BP-65 and UK-39. While crossreactivity of mAbs Sp4-7H1 and Sp4-1B4 with the antigen BP-65 was only weak, all 12 anti-sporozoite mAbs crossreacted strongly with UK-39, indicating that this compound better reflects the native structure of the CSP-repeat region.

Immunogenicity of Virosomally Formulated UK-39

Already one immunization of influenza-primed BALB/c mice with UK-39-loaded IRIVs elicited detectable titers of anti-UK-39 IgG in ELISA (Figure 5A) and sporozoite crossreactive IgG in IFA (Figure 5B). While a second immunization led to a strong titer increase, a third immunization had only a moderate further booster effect. In western blots with a lysate of *P. falciparum* salivary gland sporozoites, anti-UK-39 IgG stained a characteristic CSP double band of 50–55 kDa (data not shown).

Comparison of immune responses elicited by a liposomal and an IRIV-based formulation of UK-39 demonstrated the importance of influenza virus proteins for the immunopotentiating activity of IRIVs, in the case of UK-39 not containing any known Th epitopes in the BALB/c model [19] (Figure 5C). The strong immunogenicity of virosomally formulated UK-39 is virtually abolished when the peptide is presented on liposomes, lacking influenza-derived hemagglutinin and neuraminidase. Also, no parasite crossreactive IgG was detected in IFA (data not shown). Already one dose of IRIV-formulated UK-39 elicited high ELISA and IFA IgG titers in influenza-primed rabbits (Figure S4). Additional immunizations had only a minor booster effect. IgG from immunized animals stained the CSP double band in western blots (data not shown). IgG from sera taken 2 weeks after the third immunization (see Figure S4) was purified for sporozoite inhibition assays.

Generation of Sporozoite-Inhibitory Antibodies by UK-39

Total IgG (final concentration 1 mg/ml) purified from UK-39-immunized rabbits showed inhibitory activity in sporozoite in vitro invasion inhibition assays (Figure 6A). Inhibition decreased in a dose-dependent manner. Control IgG preparations from rabbits immunized with empty IRIVs had no inhibitory activity. Sera-inhibiting invasion of *P. falciparum* sporozoites did not inhibit invasion of *P. yoelii* into murine hepatocytes (data not shown), demonstrating specificity of the inhibitory activity.

Purified IgG from rabbits immunized with UK-39 inhibited parasite gliding motility, as demonstrated by

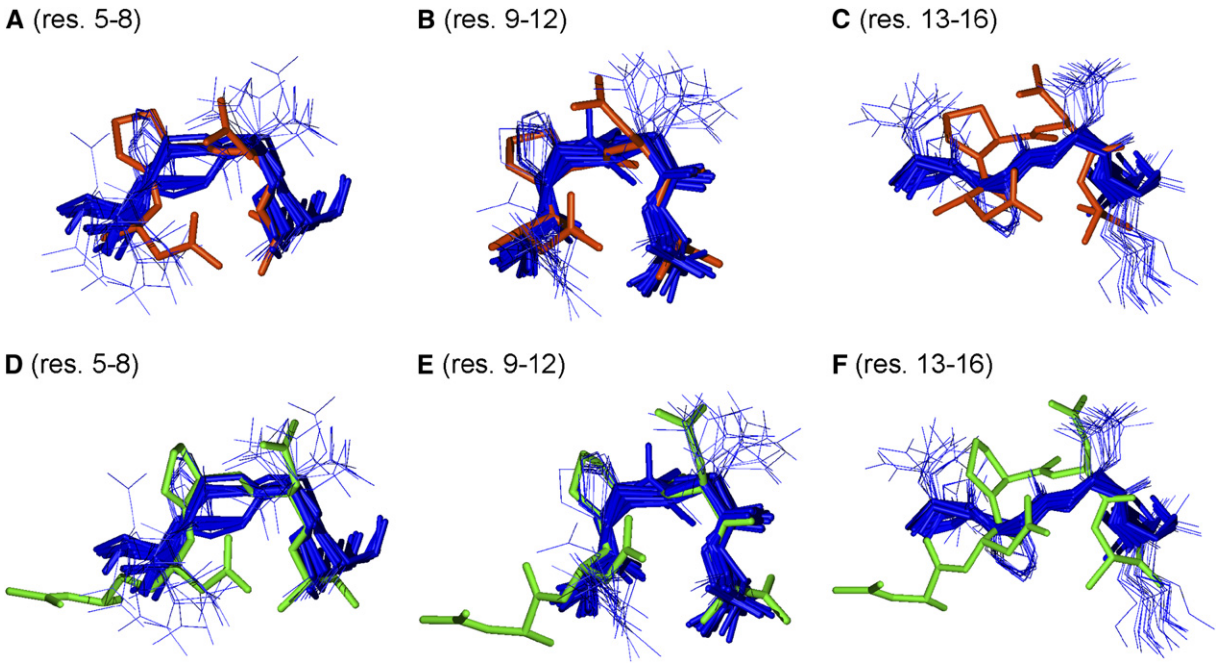

Figure 4. Backbone Superimposition of the 20 DYANA Structures of UK-40 with a Helical Turn Conformation and with the ANPNA Crystal Structure

Shown with a helical turn conformation (red, [A–C]) and with the ANPNA crystal structure (green, [D–F]).

In (A) and (D), only residues 5–8 in UK-40 were used for the superimposition, for (B) and (E), only residues 9–12, and for (C) and (F), only residues 13–16.

immunofluorescence analysis of the trails of CSP shed by *P. falciparum* sporozoites gliding on glass slides [20]. At a concentration of 1 mg/ml of total IgG, traces were reduced (Figure 6B). Furthermore, CSP was precipitated at the apical ends of the sporozoites as described [21] and sporozoites were agglutinated. Serum of rabbits immunized with empty IRIVs had no effect on gliding motility or on parasite morphology.

DISCUSSION

An important goal here was the design of a conformationally constrained peptidomimetic of the immunodominant NPNA-repeat region of CSP, which could be delivered to the immune system on the surface of IRIVs. Linear peptides are generally unsuitable as immunogens, due to their inherent conformational flexibility. As a result, there are many different ways that linear peptides can be recognized (by B cell receptors), correlating with the number of accessible conformational states available to the peptide chain. Only a small subset of these will be relevant for crossrecognition of the cognate folded protein. A peptide chain restrained into the biologically relevant backbone conformation, on the other hand, should be a more effective immunogen, as it should be recognized preferentially in a conformation that promotes crossreaction with the folded protein. There is the further advantage that linear peptides are usually degraded by proteolysis within minutes in biological fluids, which limits the window of accessibility to B cell receptors.

Our strategy for the design of a multistage multicomponent subunit malaria vaccine is to focus immune responses onto protection-relevant structural elements of key parasite proteins. Moreover, synthetic peptides and proteins with native-like folds can be presented to the immune system on IRIVs, thereby bypassing many of the problems associated with the production of stable recombinant protein-based vaccine formulations. A key parameter used for selecting vaccine candidates was the crossreactivity of elicited antibodies with the native target antigen on the cell surface of the parasite. IRIV formulations of the peptide antigens evaluated here were immunogenic in mice and rabbits. The optimized structure, UK-39, has remarkable structural and antigenic similarity with the native repeat region of the key sporozoite vaccine antigen CSP and is suitable for large-scale good manufacturing practice production.

Key structural information used to guide the design of UK-39 came from earlier NMR and modeling studies [11]. Already, NMR studies on linear peptides containing one or several tandemly linked NPNA motifs suggested the presence of turn-like structures based on the NPNA cadence, stabilized by hydrogen bonding, but in rapid dynamic equilibrium with extended chain forms [16]. Recently, an X-ray crystal structure was reported of the pentapeptide Ac-ANPNA-NH_2, which confirmed that the NPNA unit adopts a type I β turn conformation in the

Table 1. Crossreactivity of Anti-NPNA mAbs

		Crossreactivity with				
mab	Immunogen	JL-934[a]	JL-1036[a]	BP-66[a]	UK-39[a]	Sporozoites[b]
1.26[c]	JL-934[d]	+	–	–	ND	+
1.7[c]		+	–	ND	ND	–
1.15[c]		+	–	ND	ND	–
2.1[c]	JL-1036[d]	–	+	+	+	+
3.1[c]		–	+	+	+	+
3.2[c]		–	+	–	–	+
3.3[c]		–	+	+	+	+
3.4[c]		–	+	ND	ND	–
3.5[c]		–	+	ND	ND	–
EP3	BP-66[d]	–	–	+	+	+
EP9		–	+	+	+	+
Sp4-5F2	*Pf* sporozoites[e]	(+)	+	+	+	+
Sp4-2H1		(+)	+	+	+	+
Sp3-E6		–	+	+	+	+
Sp3-C6		–	(+)	+	+	+
Sp3-E9		–	(+)	+	+	+
Sp4-4B6		–	–	+	+	+
Sp4-7C2		–	–	+	+	+
Sp4-7E4		–	–	+	+	+
Sp4-7H1		–	–	(+)	+	+
Sp4-4D7		–	–	+	+	+
Sp3-B4-C12		–	–	+	+	+
Sp4-1B4		–	–	(+)	+	+

(+), weakly crossreactive; ND, not determined.
[a] ELISA reactivity to the peptides.
[b] IFA reactivity with *P. falciparum* sporozoites.
[c] Described by Moreno et al. [12].
[d] Mice were immunized with IRIVs loaded with the respective peptide.
[e] Mice were immunized with *P. falciparum* sporozoites isolated from *A. stephensi* salivary glands in Freund's adjuvant.

crystalline state [18]. Nevertheless, a key question remains how individual β turns in a longer $(NPNA)_n$ oligomer might be interconnected to form a repeat structure. In earlier work, we were strongly influenced by the observation in NOESY spectra of various $(NPNA)_n$-containing cyclic and linear peptides of strong sequential backbone NH-NH NOEs between both Asn^{i+2} and Ala^{i+3} as well as Ala^{i+3} and Asn^{i+4}. This led us to consider backbone conformations of extended $(NPNA)_n$ oligomeric peptides, in which Pro^{i+1}, Asn^{i+2}, and Ala^{i+3} are in the α-helical region, leaving only Asn^{i} in the β region of ϕ/ψ space, a combination called here a helical turn. A computer model of such a turn is shown in Figure 3A, where the close approach of the backbone amide NHs of Asn^{i+2} and Ala^{i+3} as well as Ala^{i+3} and Asn^{i+4} can be seen. With these ϕ/ψ angles for each NPNA motif, and assuming *trans* peptide bonds, a crosslinked peptidomimetic was designed using a computer model of an extended $(NPNA)_n$-oligomer, as described earlier [11]. In our first effort, (2S,3R)-3-aminoproline was used to synthesize the mimetic BP-66 and its phospholipid conjugate BP-65. Here we have investigated the related peptidomimetics UK-39 and UK-40 (Figure 1), which use instead the synthetically more accessible (2S,4S)-4-aminoproline.

NMR studies on UK-40 in aqueous solution provide insights into the preferred backbone conformations of this mimetic, and confirm a close similarity to those deduced earlier for BP-66 [11]. As expected, the residues contained within the macrocyclic ring of UK-40 are more restrained in their conformation than the NPNA units outside the macrocycle at the N and C termini (Figure 3B). The Asn^5-Ala^8 and Asn^9-Ala^{12} motifs, in particular, appear to populate helical turns, as seen in the average solution structures calculated using NOE-derived distance restraints

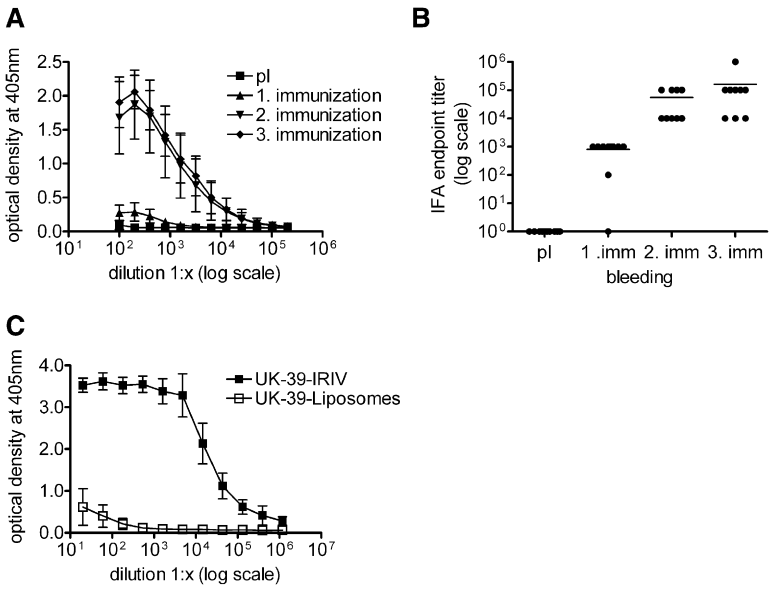

Figure 5. Immunogenicity of Virosomal and Liposomal Formulations of UK-39 in Influenza-Primed Mice

(A) Anti-UK-39 IgG response in ELISA after immunization with IRIV-formulated UK-39. Shown are mean ELISA readouts ± SD obtained with serial dilutions of mouse sera taken preimmune and 2 weeks after the first, second, and third immunizations. Sera from ten animals were analyzed at every time point.

(B) Induction of *P. falciparum* sporozoite cross-reactive IgG upon immunization with UK-39. Shown are IFA endpoint titers and geometric means of ten individual mice. Sera have been taken preimmune and 2 weeks after the first, second, and third immunizations.

(C) Anti-UK-39 IgG response in ELISA of influenza-primed mice immunized with UK-39 presented either on liposomes or on virosomes. Shown are the means ± SD of five animals per group. Sera have been taken 2 weeks after the third immunization.

(Figure 4). However, especially the Asn[13]-Glu[16] motif within the macrocycle appears to be more disordered and to exist in dynamic equilibrium with extended forms. It is less clear what role (if any) the observed minor *cis*-(Asn-Pro) peptide-bond conformers might play in eliciting antibodies crossreactive with CSP. Given that a significant population of the *cis* form exists at each Asn-Pro peptide bond, these minor conformers could play a role in antibody recognition. It would certainly be interesting to synthesize and study the immunogenicity and antigenicity of new mimetics having an increased population of *cis* tertiary amide bonds, and this will be an important focus of future work.

As far as the antigenic properties are concerned, UK-39 was recognized by all tested CSP-repeat region-specific mAbs elicited by sporozoite immunization of mice, and by the majority of sera from human donors living in malaria endemic regions (data not shown). One major limitation in using peptide antigens as vaccine components is their poor immunogenicity. We demonstrate here that presentation of UK-39 on the surface of virus-like particles elicits a strong parasite crossreactive antibody response both in mice and in rabbits. The *P. falciparum* CSP repeats are nonimmunogenic in BALB/c mice due to the lack of Th epitopes [19]. However, we were able to induce high titers of repeat-specific antibodies with virosomal formulations of UK-39. Influenza antigens on the surface of virosomes were essential to compensate for the absence of Th epitopes in the peptide, as a liposomal formulation of UK-39 was not immunogenic. We have observed better immune responses with liposomal formulations of PE conjugates of larger peptides including Th epitopes, but also in these cases, IRIV formulations were superior to liposomal formulations (unpublished results). The contribution to immunopotentiating activity of virus protein Th epitopes versus hemagglutinin-mediated endocytosis of the virosomes remains to be elucidated. In immunogenicity studies with a range of antigens, we have consistently found that preexisting anti-influenza immunity enhances the induction of antibodies against the heterologous

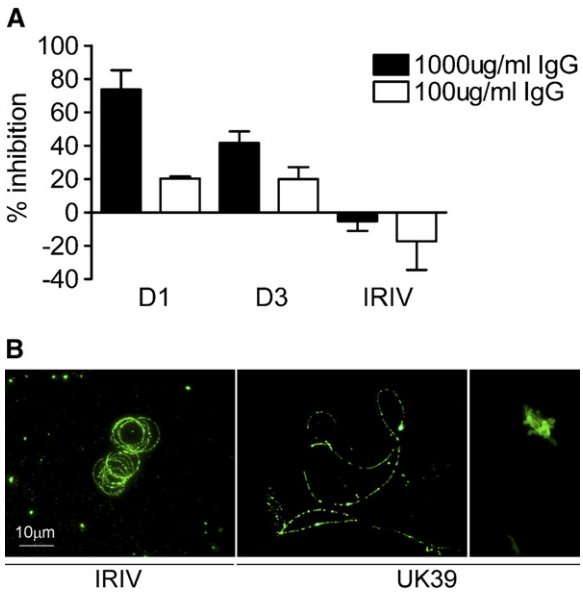

Figure 6. Inhibitory Capacity of Anti-UK-39 Antibodies

In vitro sporozoite invasion inhibition by purified rabbit IgG taken 2 weeks after the third immunization with UK-39.

(A) Shown is the mean percentage of inhibition compared to a PBS control ± SD of three experiments for two animals immunized with IRIV-formulated UK-39 (D1 and D3) and one control animal immunized with empty IRIVs (IRIV).

(B) Fluorescence microscopy of CSP trails deposited by *P. falciparum* sporozoites upon gliding on a glass slide. Left panel: trails of sporozoites incubated with purified IgG from a rabbit immunized with empty IRIVs. Middle panel: reduced trails of sporozoites incubated with purified IgG from a UK-39-immunized animal. Right panel: agglutination of sporozoites incubated with purified IgG from a rabbit immunized with UK-39.

antigens delivered on the surface of the virosomes [13, 22]. Widespread outbreaks of influenza have been reported for Africa [23], making the virosomal antigen delivery system very promising for use in malaria endemic areas of Africa.

While two immunizations were needed to reach high IgG titers in mice, one immunization was sufficient in rabbits. The observed lack of antibody boosting by additional immunizations may suggest that high titers of anti-influenza antibodies enhance clearance of the particles and reduce immunogenicity of the virosomes. However, in a phase 1 clinical trial with UK-39, no negative correlation between anti-influenza and anti-UK-39 IgG titers was found (unpublished data).

Seroconversion was not only observed in inbred mice but also in rabbits with diverse immunogenetic backgrounds. Genetic restriction of the response in humans may therefore not represent a serious limitation for IRIV-based peptide vaccines. As previously observed for other antigens [13, 22], preimmunization of animals with an influenza vaccine improved the titers of antibodies elicited by the IRIV formulation (data not shown). Possible explanations for this phenomenon are (1) opsonization of IRIVs with preexisting anti-influenza antibodies, leading to enhanced uptake by antigen-presenting cells, and (2) activation of influenza-specific memory T cells, providing T cell help to UK-39-specific B cells. The presence of antibodies against influenza is not a prerequisite for the induction of a good immune response but optimizes the adjuvant effect of virosomes [13]. Preliminary immunogenicity data of a clinical trial with two IRIV-based malaria vaccine components (B. Genton, G.P., L. Degen, A. Kammer, N. Westerfeld, S.L.O., S. Schroller, P. Vounatsou, M.S.M., M. Tanner, and R.Z., unpublished data), UK-39 and a peptide loop derived from the *P. falciparum* apical membrane antigen 1 [10], support the results obtained in experimental animals and the general concept of delivering peptides as IRIV-bound PE conjugates to the human immune system.

Antibodies against BP-65 and its easier to synthesize derivative UK-39 inhibited sporozoite invasion into hepatocytes in vitro. Inhibition with mAbs against BP-65 was up to 100%, whereas only lower levels of inhibition were observed with purified IgG from UK-39-immunized rabbits. This reduced effect can be explained by the fact that we used total IgG from immunized animals. Thus, despite using high concentrations of IgG (1 mg/ml), only a minor fraction of the antibodies is specific for the NPNA repeats. Additionally, physiological serum IgG concentrations of humans are around 12 mg/ml, pointing toward an increased inhibitory effect in vivo. Studies with purified total IgG from human volunteers immunized in a phase 1 clinical trial with UK-39 indicate that IFA titers of parasite-binding anti-UK-39 antibodies correlate very well both with sporozoite invasion and gliding inhibitory activity (S.L.O., O.S., N. Westerfeld, M. Curcic, A. Kammer, M.S.M., R.W.S., J.A.R., B. Genton, D.M., R.Z., and G.P., unpublished data).

The mechanism of sporozoite invasion inhibition is not clearly understood. The observed correlation with inhibition of gliding motility suggests interference with parasite motility, which is necessary to invade the target cell, as described before [24]. Whether this inhibition is based on a specific block of the mechanism promoting movement or just the result of steric hindrance remains to be elucidated, as the involvement of CSP in the process of gliding motility is still controversial [25]. The protective potential of anti-CSP-repeat antibodies has been shown in vivo by passive transfer of anti-CSP-repeat antibodies, which can protect mice from experimental sporozoite challenge [26]. The mechanism of this protection is at least in part due to antibody-mediated immobilization of sporozoites in the skin after injection by the mosquito [27].

It is not likely that antibodies against UK-39 alone would result in complete protection against malaria. However, in the context of a multistage vaccine, they may reduce the number of sporozoites entering liver cells and thus support immune protection elicited by components directed against the liver and blood stages of the malaria parasite. Moreover, it is thought that reduction of the number of merozoites released from the liver by anti-pre-erythrocytic vaccination [3] or reduction of the sporozoite inoculum by the use of insecticide-treated bednets [28] can reduce the incidence of severe malaria.

The universal IRIV-based antigen delivery platform described in this report is highly suitable for combining antigens specific for the different development stages of the parasite into a multicomponent malaria subunit vaccine.

SIGNIFICANCE

With increasing global prevalence of malaria and emerging resistance of *P. falciparum* to drug treatment, the need for an efficient malaria vaccine is greater than ever. Although it was shown more than 30 years ago that humans can be protected against malaria by vaccination [29], a safe, effective, and affordable vaccine is still many years away [4]. In particular, the lack of safe and potent adjuvant/delivery systems and the technical and regulatory problems associated with recombinant protein production have hampered vaccine development. We have developed a technology platform based on the design of conformationally constrained synthetic peptides and the IRIV delivery system, which allows for the rational development of a malaria vaccine. The parasite-binding capacity of antibodies elicited by immunization of mice with virosomally formulated peptides was used as a key indicator for the optimization of peptide antigens. The universal IRIV-based antigen delivery platform is highly suitable for combining antigens specific for the different development stages of the parasite into a multicomponent malaria subunit vaccine. As the IRIV system is already registered for use in humans, this platform can contribute to the rapid development of a safe, efficient, and cost-effective malaria vaccine.

EXPERIMENTAL PROCEDURES

Synthesis of Peptides

Synthesis of JL-934, JL-1036, and BP-65 has been described previously [11, 12, 30]. For UK-40, a linear peptide was first assembled on Rink amide 4-methylbenzhydrylamine resin (0.73 mM/g; Novabiochem, Nottingham, UK) using an Applied Biosystems ABI433A peptide synthesizer (Applied Biosystems, Foster City, CA), and Fmoc-protected amino acids (Fmoc-Asn[Mtt]-OH, Fmoc-Pro-OH, Fmoc-Ala-OH, Fmoc-Glu[*t*Bu]-OH, and Fmoc-[4S,2S]-4-aminoproline[Boc]-OH) and HBTU/HOBt (4 eq.) for activation. After cleavage of the linear peptide from the resin with 95% TFA, 2.5% triisopropylsilane, and 2.5% water over 3 hr, the peptide was precipitated using iPr_2O and dried. The linear peptide was then stirred overnight with HATU (4 eq.) and HOAt (4 eq.) in DMF with 1% v/v iPr_2EtN (2 mg/ml peptide). After drying in vacuo, the peptide was stirred in 20% piperidine in DMF for 15 min. The solvent was evaporated and the peptide was precipitated using iPr_2O, dried in vacuo, and then purified by reverse-phase HPLC (35% overall yield after HPLC purification; C18 column using a gradient of MeCN/H_2O [+ 0.1% TFA]; 5%–95% MeCN; t_R = 11 min). ES-MS m/z: 2276 $(M+H)^+$.

The cyclic peptide (40 mg) was coupled to PE-CO-$(CH_2)_2$-COOH (PE-succinate; 4 eq.) in DMF (5 ml), CH_2Cl_2 (5 ml), and 1% iPr_2EtN using HATU and HOAt with stirring overnight at room temperature. The solvent was then removed and the product was purified by reverse-phase HPLC (C4 column; Vydac 214 TP 1010, 25 cm × 10 mm; Vydac, Deerfield, IL) using a gradient of 50% ethanol in water to 100% ethanol (+ 0.1% TFA) over 15 min. UK-39 appears as a broad peak at about 90% ethanol; yield 15 mg (38%). ES-MS m/z: 1427 $(M+2H)^{2+}$. Alternatively, the cyclic peptide was acetylated with acetic anhydride in MeOH and NH_4HCO_3 buffer and UK-40 was purified by reverse-phase HPLC (C18 column; Vydac) using a gradient of 0%–100% MeCN in water. ES-MS m/z: 1049 $(M+2H)^{2+}$.

PE-succinate was prepared by reacting 1-palmitoyl-3-oleylphosphatidylethanolamine (400 mg, 0.57 mmol) in CH_2Cl_2/MeOH (40 ml, 9:1) with succinic anhydride (67 mg, 0.67 mmol) and Et_3N (6 eq.). After 3 hr at room temperature, the organic phase was washed, dried, and evaporated to afford the product as a white powder (450 mg, 96%). ES-MS m/z: 816.7 $(M+H)^+$.

NMR Studies

For NMR studies, UK-40 was dissolved in 90% H_2O/10% D_2O (pH 5.0) at a concentration of ca. 10 mg/ml. One- and two-dimensional ^1H NMR spectra were recorded at 600 MHz (Bruker AV-600 spectrometer; Bruker, Billerica, MA). Water suppression was by presaturation. The sequential resonance assignments were based on DQF-COSY, TOCSY, and NOESY spectra. Distance restraints were obtained from NOESY spectra with mixing times of 80 and 250 ms. Spectra were collected with 1024 × 256 complex data points zero-filled prior to Fourier transformation to 2048 × 1024, and transformed with a cosine-bell weighting function. Data processing was carried out with XWINNMR (Bruker) and XEASY [31].

The structure calculations were performed by restrained molecular dynamics in torsion angle space by applying the simulated annealing protocol implemented in the program DYANA [32]. Starting from 100 randomized conformations, a bundle of 20 conformations was selected with the lowest DYANA target energy function. The program MOLMOL [33] was used for structure analysis and visualization of the molecular models.

Preparation of Peptide-Loaded Virosomes

For the preparation of IRIVs loaded with phosphatidylethanolamine (PE)-peptide conjugates, a solution of purified Influenza A/Singapore hemagglutinin (4 mg) in phosphate-buffered saline (PBS) was centrifuged for 30 min at 100,000 × g and the pellet was dissolved in PBS (1.33 ml) containing 100 mM octaethyleneglycolmonodecylether (PBS-OEG). Peptide-PE conjugates (4 mg), phosphatidylcholine (32 mg; Lipoid, Ludwigshafen, Germany), and PE (6 mg) were dissolved in a total volume of 2.66 ml of PBS-OEG. The phospholipid and hemagglutinin solutions were mixed and sonicated for 1 min. This solution was then centrifuged for 1 hr at 100,000 × g and the supernatant was filtered (0.22 μm) under sterile conditions. Virosomes were then formed by detergent removal using Bio-Rad SM BioBeads (Bio-Rad, Glattbrugg, Switzerland). For the standardization of vaccine formulations, the content of malaria peptide antigens of the virosomes was quantified using a validated HPLC method. Furthermore, we verified that the synthetic PE-linked malaria antigens were exclusively associated with the virosomal fractions.

Mouse Immunogenicity Studies

BALB/c mice were preimmunized intramuscularly with 1 μg of purified Influenza A/Singapore hemagglutinin in 0.1 ml PBS. At least 3 weeks later, they were immunized with PE-peptide conjugate-loaded IRIVs (containing 10 μg PE-peptide) in intervals of at least 2 weeks. Blood was collected before each immunization and 2 weeks after the final injection.

Generation of Hybridomas and Production of mAbs

Hybridomas were generated from spleen cells of mice 3 days after a booster immunization with BP-65-loaded IRIVs using PAI mouse myeloma cells as a fusion partner. Hybrids were selected in hypoxanthine/aminopterin/thymidine medium and cells that secreted anti-BP-65 mAbs were identified by ELISA. For large-scale mAb production, hybridoma cell lines were cultured in 175 cm^2 flasks and mAbs were purified by protein A or G affinity chromatography (protein A Sepharose CL4B or HiTrap protein G HP; Amersham Pharmacia, Piscataway, NJ). Purified mAbs were dialyzed against PBS, aliquoted, and stored at −80°C. Generation of anti-*P. falciparum* sporozoite mAbs has been described previously [34].

Rabbit Immunogenicity Studies

Rabbits were preimmunized intramuscularly with 5 μg of purified Influenza A/Singapore hemagglutinin in 0.1 ml PBS. At least 3 weeks later, they were immunized with peptide-loaded IRIVs (containing 10 μg PE-peptide) in intervals of at least 2 weeks. Blood was collected before each immunization and 2 weeks after the final injection. Rabbit IgG was purified from immune sera (taken 2 weeks after the third immunization) by protein A affinity chromatography.

ELISA

ELISA analyses with peptide-PE conjugates were performed essentially as described before [10]. Briefly, Polysorp plates (Nunc; Fisher Scientific, Wohlen, Switzerland) were coated overnight at 4°C with 100 μl of a 10 μg/ml solution of UK-39 in PBS (pH 7.2). After three washings with PBS containing 0.05% Tween 20, wells were blocked with 5% milk powder in PBS for 30 min at 37°C and washed three times again. Plates were then incubated with serial dilutions of anti-peptide mouse or rabbit sera or anti-peptide mAbs in PBS containing 0.05% Tween 20 and 0.5% milk powder for 2 hr at 37°C. After washing, plates were incubated with alkaline phosphatase-conjugated goat anti-mouse IgG (Fc-specific) antibodies (Sigma, St. Louis, MO) for 1 hr at 37°C. After washing again, a phosphatase substrate solution (1 mg/ml *p*-nitrophenyl phosphate [Sigma] in a pH 9.8 buffer solution containing 10% [v/v] diethanolamine and 0.02% $MgCl_2$) was added and the plates were incubated in the dark at room temperature until the colorimetric reaction had progressed sufficiently. The optical density was measured at 405 nm on a Titertek Multiscan MCC/340 reader (Labsystems, Helsinki, Finland). For experiments with rabbit sera, horseradish peroxidase-conjugated goat anti-rabbit IgG heavy- and light-chain antibodies (Bio-Rad Laboratories, Hercules, CA) were used as secondary antibody. The TMB microwell peroxidase substrate system (KPL, Gaithersburg, MD) was used according to the manufacturer's protocol and the OD was measured at 650 nm. After stopping the reaction by addition of 50 μl of 1 N HCl per well, the OD was measured at 450 nm.

Indirect Immunofluorescence Assay

Air-dried unfixed *P. falciparum* (strain NF54) salivary gland sporozoites attached to microscope glass slides were incubated for 15 min at room temperature with 25 μl blocking solution containing 1% fatty acid-free bovine serum albumin in PBS. Immunostaining was performed by incubating the wells with 25 μl of an appropriate serum dilution in blocking solution in a humid chamber for 1 hr at room temperature. After five washes with blocking solution, 25 μl of 5 μg/ml cyanine dye (Cy3)-conjugated affinity-pure $F(ab')_2$ fragment goat anti-mouse IgG (Fc-specific) antibodies (Jackson Immuno Research Laboratories, West Grove, PA) or Cy3-conjugated donkey anti-rabbit IgG heavy- and light-chain antibodies (Jackson Immuno Research Laboratories), diluted in blocking solution containing 0.01 mg/ml Hoechst dye 33256 (Sigma), were added to the wells and incubated for 1 hr at room temperature. Finally, wells were washed five times with PBS, mounted with mounting solution (90% [v/v] glycerol containing 0.1 M Tris-Cl [pH 8.0] and 2 mg/ml *o*-phenylenediamine), and covered with a coverslip. Antibody binding and DNA staining were assessed by fluorescence microscopy on a Leitz Dialux 20 fluorescence microscope (Leitz, Wetzlar, Germany) and documented with a Leica DC200 digital camera system (Leica, Wetzlar, Germany).

SDS-PAGE and Immunoblotting

One hundred microliters of an *Anopheles stephensi* salivary gland lysate containing about 100,000 *P. falciparum* sporozoites was diluted with an equal volume of 2× loading buffer (1.7 ml, 0.5 M Tris-HCl [pH 6.8], 2 ml glycerol, 4.5 ml 10% SDS, 1 ml β-mercaptoethanol, 0.8 ml 0.3% [w/v] bromophenol blue) and heated to 95°C for 10 min. Proteins were separated on a 10% SDS-PAGE mini-gel. Separated proteins were electrophoretically transferred to a nitrocellulose filter (Protran nitrocellulose, BA85; Schleicher & Schuell, Bottmingen, Switzerland) by semidry blotting. Blots were blocked with PBS containing 5% milk powder and 0.1% Tween 20 overnight at 4°C. The filter was cut into strips and incubated with appropriate dilutions of immune sera in blocking buffer for 2 hr at room temperature. Filter strips were then washed three times for 10 min in blocking buffer and incubated at room temperature for 1 hr with alkaline peroxidase-conjugated goat anti-mouse IgG (Fc-specific) antibodies (Sigma) diluted 1:30,000 in blocking buffer or horseradish peroxidase-conjugated goat anti-rabbit IgG heavy- and light-chain antibodies (Bio-Rad Laboratories) diluted 1:6,000 in blocking buffer. After washing again, blots were finally developed using enhanced chemiluminescence western blotting detection (Amersham Biosciences, Buckinghamshire, UK) reagents to visualize bands.

P. falciparum and *P. yoelii* In Vitro Invasion Inhibition Assay

Inhibition assays were performed as described before [35, 36]. Briefly, primary human or mouse hepatocytes were isolated as described [37, 38], and inoculated with *P. falciparum* (NF54 strain) or *P. yoelii* (265BY strain) sporozoites (1 × 105/Labtek well) obtained from salivary glands of infected *A. stephensi* mosquitoes. After 3 hr at 37°C, the cultures were washed, and further incubated in fresh medium for 3 days (*P. falciparum*) or 2 days (*P. yoelii*) before fixation in methanol. Quantification of exoerythrocytic forms was done by immunofluorescence. To determine the effects of anti-CSP antibodies on sporozoite infectivity, sporozoites were incubated with hepatocytes in the presence of increasing concentrations of mAbs or purified polyclonal rabbit IgG from immunized animals. The percentage of inhibition was determined in comparison to a PBS control.

Gliding Inhibition

To analyze sporozoite motility, 30,000 sporozoites were deposited on multispot glass slide wells precoated with anti-*P. falciparum* CSP (*Pf*CSP) mAb E9 (100 μg/ml, 1 hr at 37°C) and incubated at 37°C for 1 hr. The slides were then washed, and the deposited CSP trails were fixed with 4% paraformaldehyde for 15 min. The trails were then labeled using the anti-*Pf*CSP mAb E9 conjugated to Alexa Fluor 488 and visualized under a fluorescence microscope.

Supplemental Data

Supplemental Data include four figures and two tables and are available at http://www.chembiol.com/cgi/content/full/14/5/577/DC1/.

ACKNOWLEDGMENTS

We thank G.J. van Gemert, J.F. Franetich, T. Houpert, and L. Hannoun for their contribution to this study. This project was cofinanced by the Commission for Technology and Innovation (BBT, Switzerland). R.Z. is an employee of Pevion Biotech Ltd.

Received: October 16, 2006
Revised: March 13, 2007
Accepted: April 2, 2007
Published: May 29, 2007

REFERENCES

1. Snow, R.W., Guerra, C.A., Noor, A.M., Myint, H.Y., and Hay, S.I. (2005). The global distribution of clinical episodes of *Plasmodium falciparum* malaria. Nature *434*, 214–217.
2. Targett, G.A. (2005). Malaria vaccines 1985–2005: a full circle? Trends Parasitol. *21*, 499–503.
3. Alonso, P.L., Sacarlal, J., Aponte, J.J., Leach, A., Macete, E., Milman, J., Mandomando, I., Spiessens, B., Guinovart, C., Espasa, M., et al. (2004). Efficacy of the RTS,S/AS02A vaccine against *Plasmodium falciparum* infection and disease in young African children: randomised controlled trial. Lancet *364*, 1411–1420.
4. Greenwood, B. (2005). Malaria vaccines. Evaluation and implementation. Acta Trop. *95*, 298–304.
5. Greenwood, B.M., Bojang, K., Whitty, C.J., and Targett, G.A. (2005). Malaria. Lancet *365*, 1487–1498.
6. Waters, A. (2006). Malaria: new vaccines for old? Cell *124*, 689–693.
7. Luke, T.C., and Hoffman, S.L. (2003). Rationale and plans for developing a non-replicating, metabolically active, radiation-attenuated *Plasmodium falciparum* sporozoite vaccine. J. Exp. Biol. *206*, 3803–3808.
8. Good, M.F. (2005). Vaccine-induced immunity to malaria parasites and the need for novel strategies. Trends Parasitol. *21*, 29–34.
9. Tongren, J.E., Zavala, F., Roos, D.S., and Riley, E.M. (2004). Malaria vaccines: if at first you don't succeed… Trends Parasitol. *20*, 604–610.
10. Mueller, M.S., Renard, A., Boato, F., Vogel, D., Naegeli, M., Zurbriggen, R., Robinson, J.A., and Pluschke, G. (2003). Induction of parasite growth-inhibitory antibodies by a virosomal formulation of a peptidomimetic of loop I from domain III of *Plasmodium falciparum* apical membrane antigen 1. Infect. Immun. *71*, 4749–4758.
11. Pfeiffer, B., Peduzzi, E., Moehle, K., Zurbriggen, R., Gluck, R., Pluschke, G., and Robinson, J.A. (2003). A virosome-mimotope approach to synthetic vaccine design and optimization: synthesis, conformation, and immune recognition of a potential malaria-vaccine candidate. Angew. Chem. Int. Ed. Engl. *42*, 2368–2371.
12. Moreno, R., Jiang, L., Moehle, K., Zurbriggen, R., Gluck, R., Robinson, J.A., and Pluschke, G. (2001). Exploiting conformationally constrained peptidomimetics and an efficient human-compatible delivery system in synthetic vaccine design. ChemBioChem *2*, 838–843.
13. Poltl-Frank, F., Zurbriggen, R., Helg, A., Stuart, F., Robinson, J., Gluck, R., and Pluschke, G. (1999). Use of reconstituted influenza virus virosomes as an immunopotentiating delivery system for a peptide-based vaccine. Clin. Exp. Immunol. *117*, 496–503.
14. Zurbriggen, R. (2003). Immunostimulating reconstituted influenza virosomes. Vaccine *21*, 921–924.

15. Herrington, D.A., Clyde, D.F., Losonsky, G., Cortesia, M., Murphy, J.R., Davis, J., Baqar, S., Felix, A.M., Heimer, E.P., Gillessen, D., et al. (1987). Safety and immunogenicity in man of a synthetic peptide malaria vaccine against *Plasmodium falciparum* sporozoites. Nature *328*, 257–259.

16. Dyson, H.J., Satterthwait, A.C., Lerner, R.A., and Wright, P.E. (1990). Conformational preferences of synthetic peptides derived from the immunodominant site of the circumsporozoite protein of *Plasmodium falciparum* by ^{1}H NMR. Biochemistry *29*, 7828–7837.

17. Wüthrich, K. (1986). NMR of Proteins and Nucleic Acids (New York: John Wiley & Sons).

18. Ghasparian, A., Moehle, K., Linden, A., and Robinson, J.A. (2006). Crystal structure of an NPNA-repeat motif from the circumsporozoite protein of the malaria parasite *Plasmodium falciparum*. Chem. Commun. (Camb.), 174–176.

19. Good, M.F., Berzofsky, J.A., Maloy, W.L., Hayashi, Y., Fujii, N., Hockmeyer, W.T., and Miller, L.H. (1986). Genetic control of the immune response in mice to a *Plasmodium falciparum* sporozoite vaccine. Widespread nonresponsiveness to single malaria T epitope in highly repetitive vaccine. J. Exp. Med. *164*, 655–660.

20. Stewart, M.J., and Vanderberg, J.P. (1988). Malaria sporozoites leave behind trails of circumsporozoite protein during gliding motility. J. Protozool. *35*, 389–393.

21. Vanderberg, J.P. (1974). Studies on the motility of *Plasmodium* sporozoites. J. Protozool. *21*, 527–537.

22. Zurbriggen, R., and Gluck, R. (1999). Immunogenicity of IRIV-versus alum-adjuvanted diphtheria and tetanus toxoid vaccines in influenza primed mice. Vaccine *17*, 1301–1305.

23. Montefiore, D., Drozdov, S.G., Kafuko, G.W., Fayinka, O.A., and Soneji, A. (1970). Influenza in East Africa, 1969–70. Bull. World Health Organ. *43*, 269–273.

24. Stewart, M.J., Nawrot, R.J., Schulman, S., and Vanderberg, J.P. (1986). *Plasmodium berghei* sporozoite invasion is blocked in vitro by sporozoite-immobilizing antibodies. Infect. Immun. *51*, 859–864.

25. Kappe, S.H., Buscaglia, C.A., and Nussenzweig, V. (2004). *Plasmodium* sporozoite molecular cell biology. Annu. Rev. Cell Dev. Biol. *20*, 29–59.

26. Yoshida, N., Nussenzweig, R.S., Potocnjak, P., Nussenzweig, V., and Aikawa, M. (1980). Hybridoma produces protective antibodies directed against the sporozoite stage of malaria parasite. Science *207*, 71–73.

27. Vanderberg, J.P., and Frevert, U. (2004). Intravital microscopy demonstrating antibody-mediated immobilisation of *Plasmodium berghei* sporozoites injected into skin by mosquitoes. Int. J. Parasitol. *34*, 991–996.

28. Nevill, C.G., Some, E.S., Mung'ala, V.O., Mutemi, W., New, L., Marsh, K., Lengeler, C., and Snow, R.W. (1996). Insecticide-treated bednets reduce mortality and severe morbidity from malaria among children on the Kenyan coast. Trop. Med. Int. Health *1*, 139–146.

29. Clyde, D.F., Most, H., McCarthy, V.C., and Vanderberg, J.P. (1973). Immunization of man against sporozoite-induced falciparum malaria. Am. J. Med. Sci. *266*, 169–177.

30. Bisang, C., Jiang, L., Freund, E., Emery, F., Bauch, C., Matile, H., Pluschke, G., and Robinson, J.A. (1998). Synthesis, conformational properties, and immunogenicity of a cyclic template-bound peptide mimetic containing an NPNA motif from the circumsporozoite protein of *Plasmodium falciparum*. J. Am. Chem. Soc. *120*, 7439–7449.

31. Bartels, C., Xia, T.-h., Billeter, M., Güntert, P., and Wüthrich, K. (1995). The program XEASY for computer-supported NMR spectral analysis of biological macromolecules. J. Biomol. NMR *6*, 1–10.

32. Güntert, P., Mumenthaler, C., and Wüthrich, K. (1997). Torsion angle dynamics for NMR structure calculation with the new program DYANA. J. Mol. Biol. *273*, 283–298.

33. Koradi, R., Billeter, M., and Wüthrich, K. (1996). MOLMOL: a program for display and analysis of macromolecular structures. J. Mol. Graph. *14*, 29–32, 51–55.

34. Stuber, D., Bannwarth, W., Pink, J.R., Meloen, R.H., and Matile, H. (1990). New B cell epitopes in the *Plasmodium falciparum* malaria circumsporozoite protein. Eur. J. Immunol. *20*, 819–824.

35. Mazier, D., Mellouk, S., Beaudoin, R.L., Texier, B., Druilhe, P., Hockmeyer, W., Trosper, J., Paul, C., Charoenvit, Y., Young, J., et al. (1986). Effect of antibodies to recombinant and synthetic peptides on *P. falciparum* sporozoites in vitro. Science *231*, 156–159.

36. Silvie, O., Franetich, J.F., Charrin, S., Mueller, M.S., Siau, A., Bodescot, M., Rubinstein, E., Hannoun, L., Charoenvit, Y., Kocken, C.H., et al. (2004). A role for apical membrane antigen 1 during invasion of hepatocytes by *Plasmodium falciparum* sporozoites. J. Biol. Chem. *279*, 9490–9496.

37. Mazier, D., Beaudoin, R.L., Mellouk, S., Druilhe, P., Texier, B., Trosper, J., Miltgen, F., Landau, I., Paul, C., Brandicourt, O., et al. (1985). Complete development of hepatic stages of *Plasmodium falciparum* in vitro. Science *227*, 440–442.

38. Renia, L., Mattei, D., Goma, J., Pied, S., Dubois, P., Miltgen, F., Nussler, A., Matile, H., Menegaux, F., Gentilini, M., et al. (1990). A malaria heat-shock-like determinant expressed on the infected hepatocyte surface is the target of antibody-dependent cell-mediated cytotoxic mechanisms by nonparenchymal liver cells. Eur. J. Immunol. *20*, 1445–1449.